



Spray-Drying Synthesis of LiFeBO₃/C Hollow Spheres With Improved Electrochemical and Storage Performances for Li-Ion Batteries

Yulei Sui¹, Wei Chen¹, Shibao Tang¹, Ling Wu^{1*}, Binjue Wang¹, Huacheng Li², Wei Li³ and Shengkui Zhong^{1*}

¹ School of Iron and Steel, Soochow University, Suzhou, China, ² Citic Dameng Mining Industries Limited, Chongzuo, China, ³ Guangxi Key Laboratory of Electrochemical and Magnetochemical Functional Materials, Guilin University of Technology, Guilin, China

OPEN ACCESS

Edited by:

Juchen Guo,
University of California, Riverside,
United States

Reviewed by:

Qiaobao Zhang,
Xiamen University, China
Biao Gao,
Wuhan University of Science and
Technology, China

*Correspondence:

Ling Wu
lwu@suda.edu.cn
Shengkui Zhong
zhongshengkui@suda.edu.cn

Specialty section:

This article was submitted to
Electrochemistry,
a section of the journal
Frontiers in Chemistry

Received: 29 March 2019

Accepted: 09 May 2019

Published: 28 May 2019

Citation:

Sui Y, Chen W, Tang S, Wu L, Wang B, Li H, Li W and Zhong S (2019) Spray-Drying Synthesis of LiFeBO₃/C Hollow Spheres With Improved Electrochemical and Storage Performances for Li-Ion Batteries. *Front. Chem.* 7:379. doi: 10.3389/fchem.2019.00379

LiFeBO₃/C cathode material with hollow sphere architecture is successfully synthesized by a spray-drying method. SEM and TEM results demonstrate that the micro-sized LiFeBO₃/C hollow spheres consist of LiFeBO₃@C particles and the average size of LiFeBO₃@C particles is around 50–100 nm. The thickness of the amorphous carbon layer which is coated on the surface of LiFeBO₃ nanoparticles is about 2.5 nm. LiFeBO₃@C particles are connected by carbon layers and formed conductive network in the LiFeBO₃/C hollow spheres, leading to improved electrical conductivity. Meanwhile, the hollow structure boosts the Li⁺ diffusion and the carbon layers of LiFeBO₃@C particles protect LiFeBO₃ from moisture corrosion. Consequently, synthesized LiFeBO₃/C sample exhibits good electrochemical properties and storage performance.

Keywords: Li-ion batteries, LiFeBO₃, hollow sphere, cathode materials, spray drying

INTRODUCTION

With the development of electric vehicles in the twenty-first century, Li-ion batteries (LIBs) play an increasingly important role in modern society (Nayak et al., 2018; Wu et al., 2019) and various cathode materials are developed (Ma et al., 2015; Zheng et al., 2018a,b; Yang et al., 2019). Recently, borate-based materials (LiMBO₃, M = Fe, Mn, and Co) have received wide attention in the field of LIBs (Lin et al., 2012; Tao et al., 2013). Compared with the commonly used phosphate-based materials (LiMPO₄, M = Fe, Mn, and Co), borate groups (LiMBO₃, M = Fe, Mn, and Co) with a low specific weight show higher capacities. For instance, the theoretical capacity of LiMnBO₃ is 222 mAh g⁻¹, whereas the phosphate counterpart, LiMnPO₄, is limited to 170 mAh g⁻¹ (Moskon et al., 2016; Zhang et al., 2017). Moreover, the volume changes of borate-based materials during charging-discharging process are less than those of phosphate-based materials so that they usually show good structural stability (Loftager et al., 2017). Among various borate-based cathode materials, LiFeBO₃ with the theoretical capacity of 220 mAh g⁻¹ presents moderate working voltage, relatively high intrinsic conductivity, and good structural stability (Michalski et al., 2017). Therefore, LiFeBO₃ is considered as a potential cathode material for LIBs. However, there is only one-dimensional (1D) pathway for Li⁺ diffusing in the LiFeBO₃ crystal, which leading to low electronic and ionic conductivity (Dong et al., 2008; Kalantarian et al., 2013). Furthermore, LiFeBO₃ is highly sensitive to moisture so that surface poisoning by H₂O molecules of air would seriously disrupt its electrochemical properties (Gu et al., 2017). These problems make it

challenging to achieve LiFeBO₃-based materials with high reversible specific capacity and good storage performance. In order to improve the electrochemical performance of LiFeBO₃-based materials, various strategies have been introduced, such as metal-ions doping, conductive carbon coating, and nano-architecturing (Aravindan and Umadevi, 2012; Afyon et al., 2013; Le Roux et al., 2015; Sin et al., 2015). Among these methods, carbon coating is a promising and effective way to improve

the properties of LiFeBO₃, which attributes to the improved conductivity and the prevention of moisture corrosion. For example, Li et al. reported that the carbon coated LiFeBO₃ nanoparticles exhibit the improved first discharge capacities of 190.4 and 106.6 mAh g⁻¹ at 0.1 and 1°C rate, respectively (Li et al., 2015). The LiFeBO₃/C prepared by Zhang et al. also indicated carbon coating is an effective way to improve the properties of LiFeBO₃. However, the rate capability and storage performance of LiFeBO₃ are still not satisfied (Zhang et al., 2014). Therefore, achieving homogeneous carbon coated LiFeBO₃ cathode materials with high electrochemical properties and good storage performance is still a challenge right now.

Herein, LiFeBO₃/C with hollow porous sphere architecture is successfully synthesized by spray-drying method at the temperature as low as 450°C (Li et al., 2015). Amorphous carbon layer which was produced by polyethylene glycol 6,000 (PEG-6000) decomposition is coated on the surface of LiFeBO₃ nanoparticles. The LiFeBO₃@C particles are connected together and formed LiFeBO₃/C hollow porous spheres. The obtained LiFeBO₃/C sample with distinctive architecture shows the improved electrochemical and storage performances as cathode for LIBs.

EXPERIMENTAL

Synthesis of LiFeBO₃/C and LiFeBO₃

Firstly, LiNO₃, 1.38g LiNO₃, 8.08g Fe(NO₃)₃·9H₂O, and 1.24g H₃BO₃ were weighed and dissolved gradually in deionized water under stirring, and the mixed solution was named solution A. Meanwhile, 1.22 g PEG-6000 was dropped and dissolved in deionized water under stirring to form solution B. Then the solution B was added into the solution A and stirred carefully. A homogeneous sol was obtained when the mixed solution has been stirred at 80°C for 1 h. The precursor of LiFeBO₃/C was synthesized using the obtained sol as raw material via a spray drying process. The inlet and outlet air temperatures are 200 and

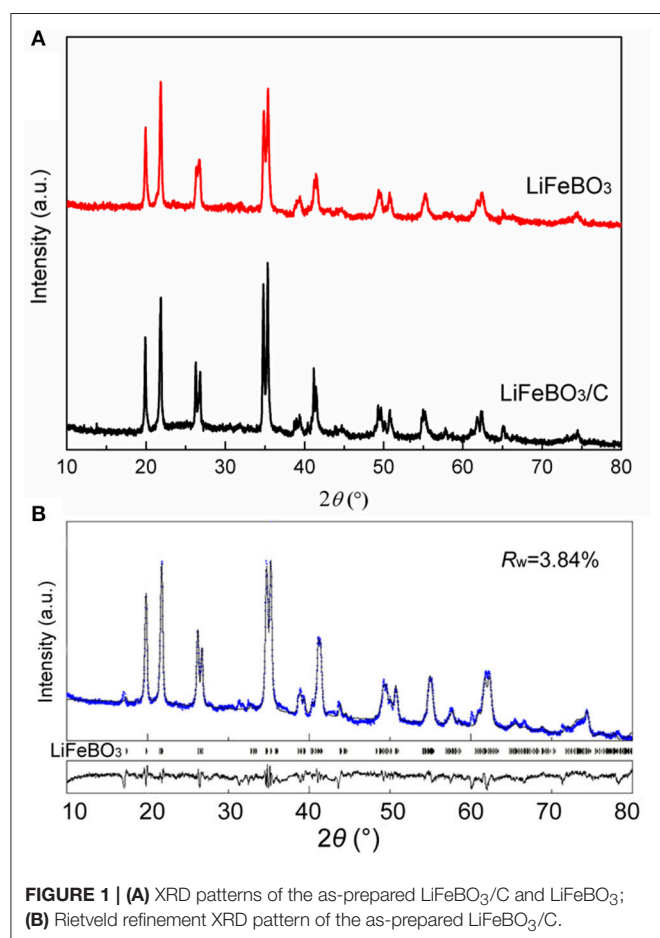


FIGURE 1 | (A) XRD patterns of the as-prepared LiFeBO₃/C and LiFeBO₃; **(B)** Rietveld refinement XRD pattern of the as-prepared LiFeBO₃/C.

TABLE 1 | Results of structural analysis obtained from X-ray Rietveld refinement of LiFeBO₃/C.

Atom	Site	x	Y	z	Occupancy
Li1	8f	0.6175	0.5429	0.1539	0.48
Li2	8f	0.6573	0.4782	0.0605	0.52
Fe1	8f	0.1372	0.3332	0.1392	0.72
Fe2	8f	0.1835	0.3435	0.0915	0.28
B1	8f	0.1592	0.6431	0.1043	1
O1	8f	0.3877	0.1737	0.0891	1
O2	8f	0.7673	0.3031	0.1497	1
O3	8f	0.3229	0.5376	0.1216	1
Lattice parameters		a (Å)	b (Å)	c (Å)	β (°)
Sample		5.1662	8.9141	10.1700	91.25

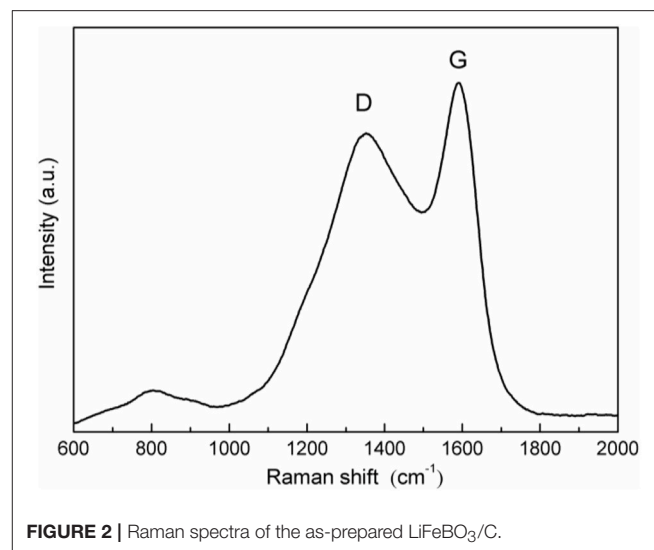


FIGURE 2 | Raman spectra of the as-prepared LiFeBO₃/C.

100°C during the spray drying process with the air pressure of 0.25 MPa. The as-obtained precursor was calcined at 350°C (3 h), followed by crystallized at 450°C for 10 h in an argon atmosphere, and the final LiFeBO₃/C was obtained. For contrast, the LiFeBO₃ sample was also prepared by the similar synthetic process but without PEG-6000. All the chemical reagents employed in this work were of analytic grade.

Characterization

The structure of LiFeBO₃/C and LiFeBO₃ samples was investigated by XRD (Rigaku/Ultima-IV) and Raman microspectroscopy. And the range of XRD and Raman spectroscopic analysis is $2\theta = 10 \sim 80^\circ$ and 600–2,000 cm⁻¹, respectively. Morphology and microstructure of LiFeBO₃/C and LiFeBO₃ samples were investigated by SEM (JSM/6380LV) and TEM

(TecnaiG220). C-S analysis (Eltar) was used to determine the carbon content of samples.

Electrochemical Measurements

The electrochemical measurements were performed in coin-type cells (CR2025) with lithium metal as the negative electrode. The positive electrodes were prepared by mixing as-prepared LiFeBO₃/C or LiFeBO₃ powder, acetylene black (99.9%, Sinopharm Chemical Reagent Co., Ltd.) and polyvinylidene fluoride (PVDF, 99.9%, Sinopharm Chemical Reagent Co., Ltd. the weight ratio is 80:10:10) in N-methylpyrrolone onto an Al foil and dried at 120°C for 4 h in vacuum oven. Then the coin-type cells were assembled in a glove box filled with high purity argon. 1M LiPF₆ solution in a mixture of ethylene carbonate and dimethyl carbonate with 1:1 volumetric ratio was used as electrolyte (Sinopharm Chemical Reagent Co., Ltd.). The cells

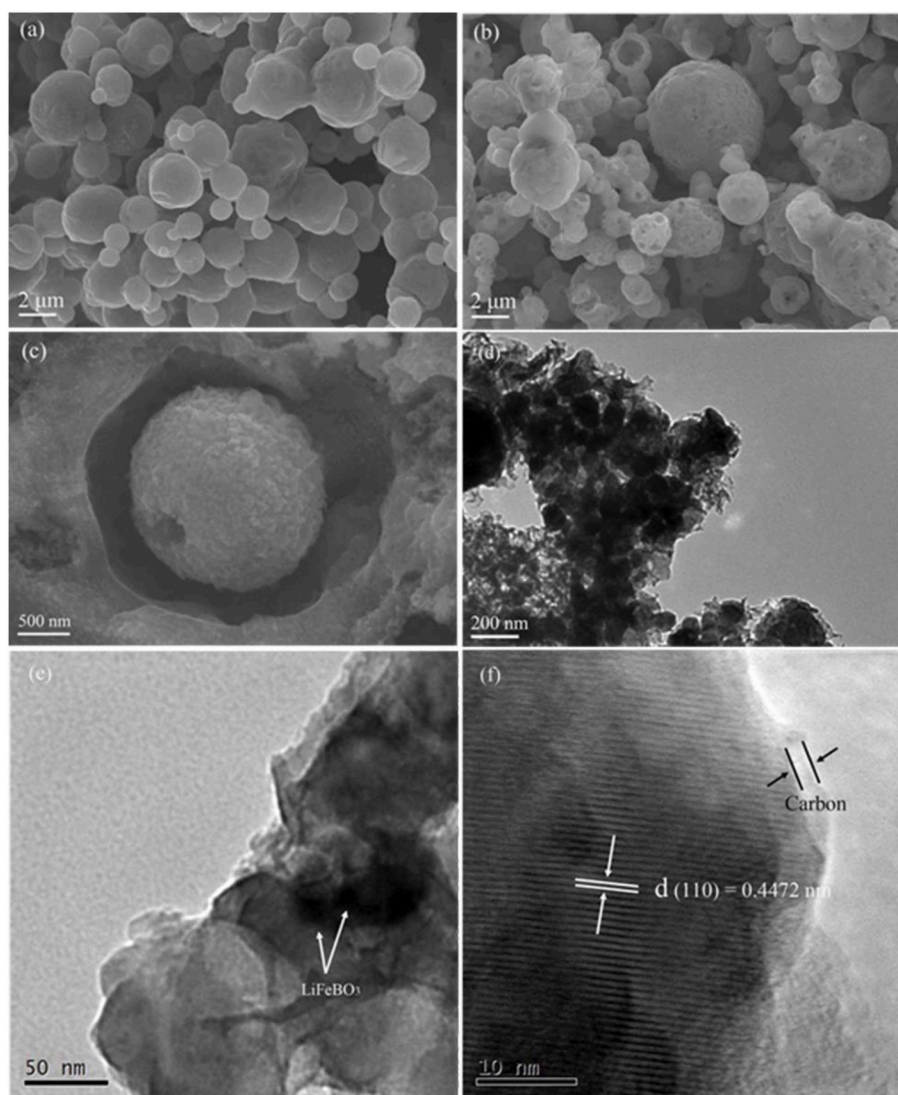
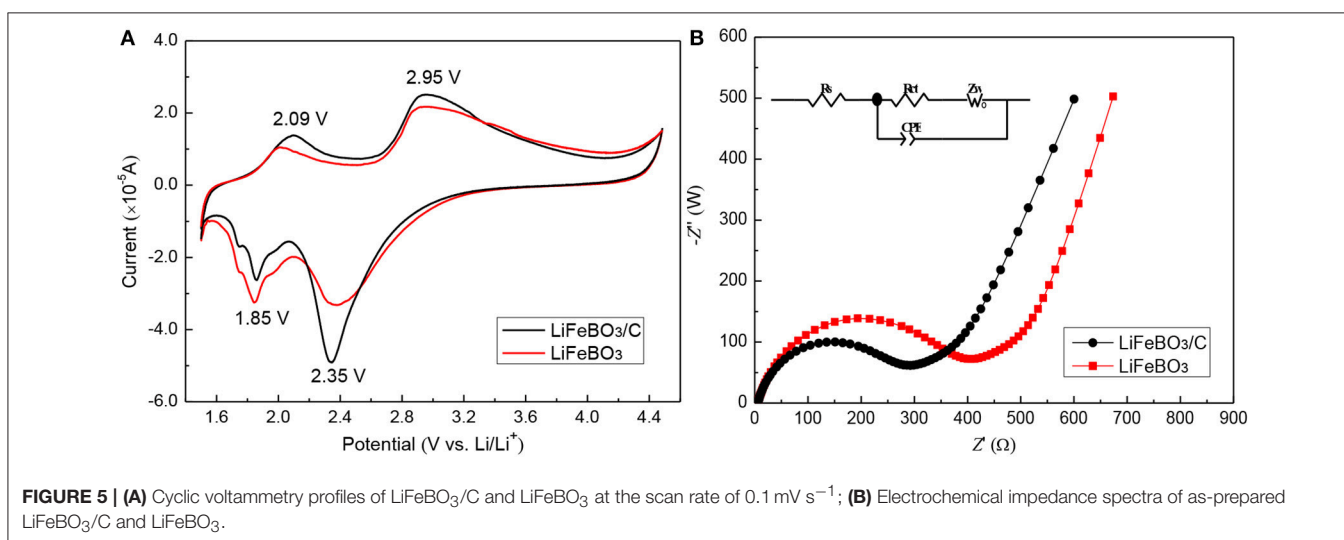
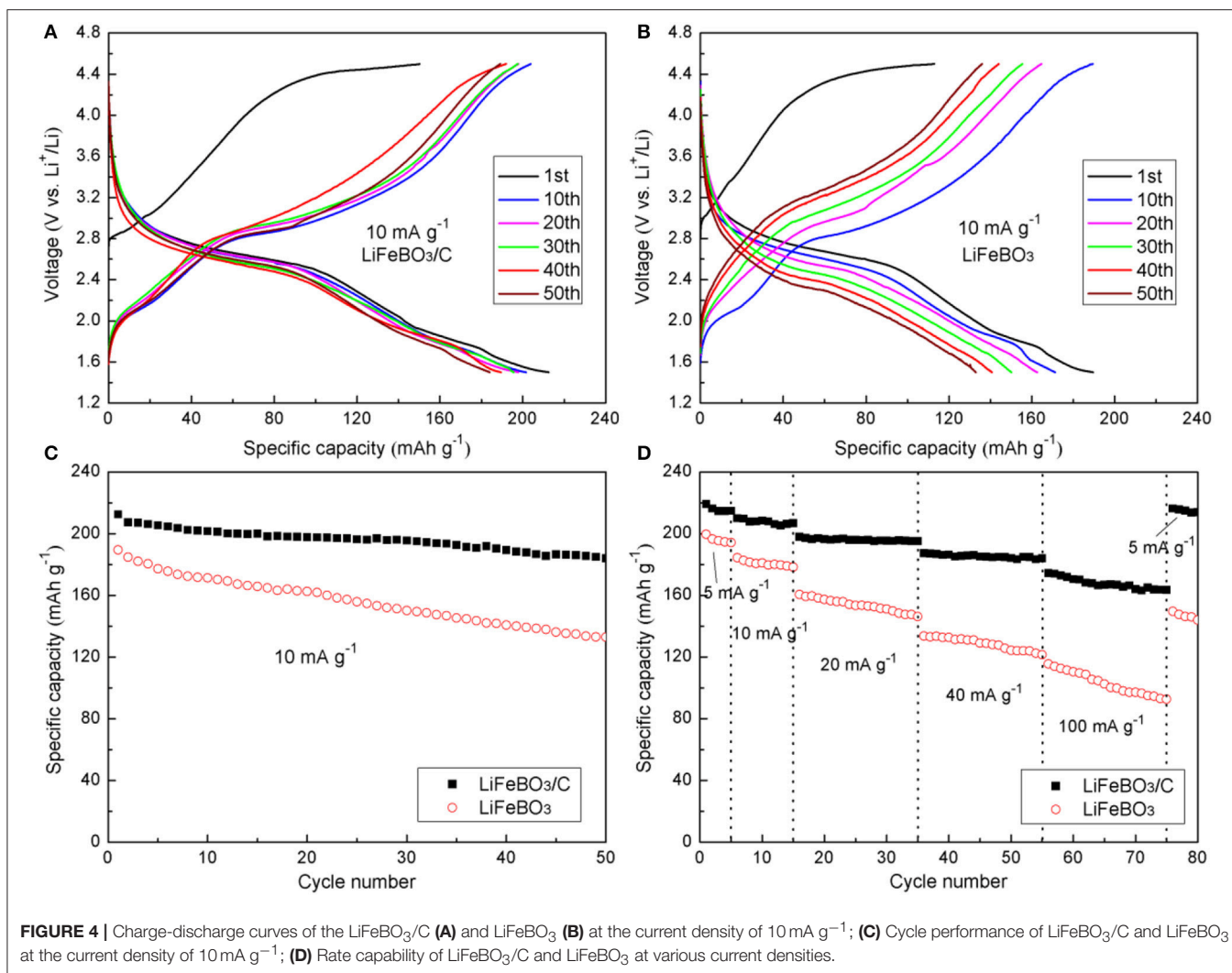


FIGURE 3 | SEM images of the as-prepared LiFeBO₃ (a) and LiFeBO₃/C (b,c); TEM images of the as-prepared LiFeBO₃/C (d-f).



were tested in the voltage range of 1.5–4.5 V under various charge/discharge current densities from 5 to 100 mA g⁻¹ at room temperature. The electrochemical impedance spectroscopy (EIS) and the cyclic voltammetry (CV) was both measured by a CHI 660D workstation.

RESULTS AND DISCUSSION

XRD patterns of the synthesized LiFeBO₃/C and LiFeBO₃ samples are shown in **Figure 1A**. Obviously, the LiFeBO₃ with monoclinic structure is well-crystallized. XRD patterns of two samples are similar, indicating the combination of LiFeBO₃ and carbon has little influence on the crystal structure. Although the amount of carbon in the LiFeBO₃/C composites is 4.9 wt. % (proved by C-S analysis), the diffraction peak of carbon is not detected from the XRD patterns, implying the carbon in the LiFeBO₃/C composite is amorphous.

In order to further clarify the crystal structure and lattice parameters of the synthesized LiFeBO₃/C, XRD data was refined by Rietveld method (Rietveld, 1967) using Maud software (Lutterotti, 2011), and the Rietveld refinement XRD pattern and atoms positions and occupancy for Li and Fe atoms in LiFeBO₃/C investigated. As can be seen from **Figure 1B** and **Table 1**, the sharp peaks of the sample can be identified as monoclinic LiFeBO₃ with space group of C2/c and the structure is crystallized well. Meanwhile, the observed and calculated patterns match well, and the reliability factors are good. In accordance with the refinement results, the lattice parameters of LiFeBO₃ are $a = 5.1662 \text{ \AA}$, $b = 8.9141 \text{ \AA}$, $c = 10.1700 \text{ \AA}$, $\beta = 91.25^\circ$, agreeing well with the reported literature (Zhang et al., 2014).

Figure 2 represents the Raman spectroscopy of the as-prepared LiFeBO₃/C sample. As can be seen from **Figure 2**, the broad peak observed at 1,354 cm⁻¹ correspond to the D (disordered) band of carbon while the broad peak located at 1,590 cm⁻¹ agreeing well with G (graphitized) band of sp² type carbon (Liu et al., 2015; Zhu et al., 2017). The strong D-peak further reveals that the carbon is amorphous, which is in agreement with the XRD result.

SEM and TEM were employed to analyze morphology and micro-structure of the synthesized LiFeBO₃ and LiFeBO₃/C. As shown in **Figure 3a**, the LiFeBO₃ sample displays a spherical shape with a size distribution in the range of 1–4 μm and the surface is compact. While, the LiFeBO₃/C sample exhibits hollow spherical shape with a rough and porous surface layer (**Figures 3b,c**). The comparison of the darker outer shell and the lighter central regions indicates that the LiFeBO₃/C spheres present porous and hollow internal structure (**Figure 3d**), which

is consistent with the SEM results. As shown in **Figure 3c**, it is obvious that the spherical LiFeBO₃/C are actually consist of numerous primary nanoparticles. **Figure 3e** shows that nano-sized primary LiFeBO₃ particles are well wrapped by thick carbon layer. This carbon-coated layer is benefit to prevent LiFeBO₃ from moisture corrosion. As we can see from **Figure 3f**, the lattice fringe with an interior planar distance of 0.4472 nm is correspond well to (1 1 0) crystal planes of LiFeBO₃. The coating layer with the thickness of 2.5 nm could be assigned to the amorphous carbon, so that LiFeBO₃@C shows a core-shell structure. In addition, the carbon-coated layer and conductive carbon network can improve the conductivity of LiFeBO₃-based cathode material, which is also benefit to the electrochemical performances.

In the potential (vs. Li/Li⁺) range of 1.5–4.5 V, the cells were charged/discharged at 10 mA g⁻¹, and the curves of the as-synthesized LiFeBO₃/C and LiFeBO₃ samples are exhibited in **Figures 4A,B**, respectively. It is noted that the initial charge curves of both samples show obviously higher voltage plateau than the subsequent cycles, which mainly due to the high polarization before cycling. This phenomenon is very similar to cases of LiMnBO₃ and LiCoBO₃ (Afyon et al., 2014; Tang et al., 2015). The charge plateau (~3.2 V) and the discharge plateau (~2.8 V) in the voltage profiles correspond to the plateaus of LiFeBO₃. There is a reduced thermodynamic potential for the degraded LiFeBO₃ phase so that a short discharge plateau ~1.8 V appeared in the discharge profiles (Bo et al., 2012).

The cycling performances of the as-prepared LiFeBO₃/C and LiFeBO₃ samples at 10 mA g⁻¹ are shown in **Figure 4C**. The initial discharge specific capacities of LiFeBO₃/C and LiFeBO₃ are 212.4 and 189.5 mAh g⁻¹, respectively. The specific capacity of LiFeBO₃/C is as high as 184.1 mAh g⁻¹ while the specific capacity of LiFeBO₃ is only 132.9 mAh g⁻¹ after 50 cycles, indicating the LiFeBO₃/C sample has a better cyclic stability. **Figure 4D** displays the rate capability of the as-prepared LiFeBO₃/C and LiFeBO₃ samples under different current densities. The initial capacity of the as-prepared LiFeBO₃/C is 219.2 mAh g⁻¹ at 5 mA g⁻¹, which is approximately 98.7% of the theoretical capacity. When the current density is increased up to 40 and 100 mA g⁻¹, the LiFeBO₃/C sample holds a stable reversible capacity of 187.3 and 175.8 mAh g⁻¹, respectively. However, the discharge capacity of LiFeBO₃ at 40 and 100 mA g⁻¹ are only 144.5 and 115.5 mAh g⁻¹, respectively. If the current density returns back to 5 mA g⁻¹ after 75 cycles test, and 98.6% of the initial discharge specific capacity (216.3 mAh g⁻¹) can be recovered for LiFeBO₃/C but only 75.1% was recovered for LiFeBO₃ electrode (149.6 mAh g⁻¹), implying the LiFeBO₃/C sample has a better capacity recovery ability than LiFeBO₃. The improved electrochemical performances can be attributed to the special hollow sphere structure and network of amorphous carbon layer. The conductivity is improved by the network of amorphous carbon layer and the volume expansion during the charge and discharge progresses is againted due to the special hollow sphere architecture provides a flexible structure, so that the electrochemical performance of the synthesized cathode is improved (Li et al., 2013).

TABLE 2 | Parameters obtained from equivalent circuit fitting of EIS data.

Sample	$R_s(\Omega)$	$R_{ct}(\Omega)$	$j_o(\text{mA cm}^{-2})$
LiFeBO ₃	6.03	354.12	7.26×10^{-5}
LiFeBO ₃ /C	5.79	238.60	10.78×10^{-5}

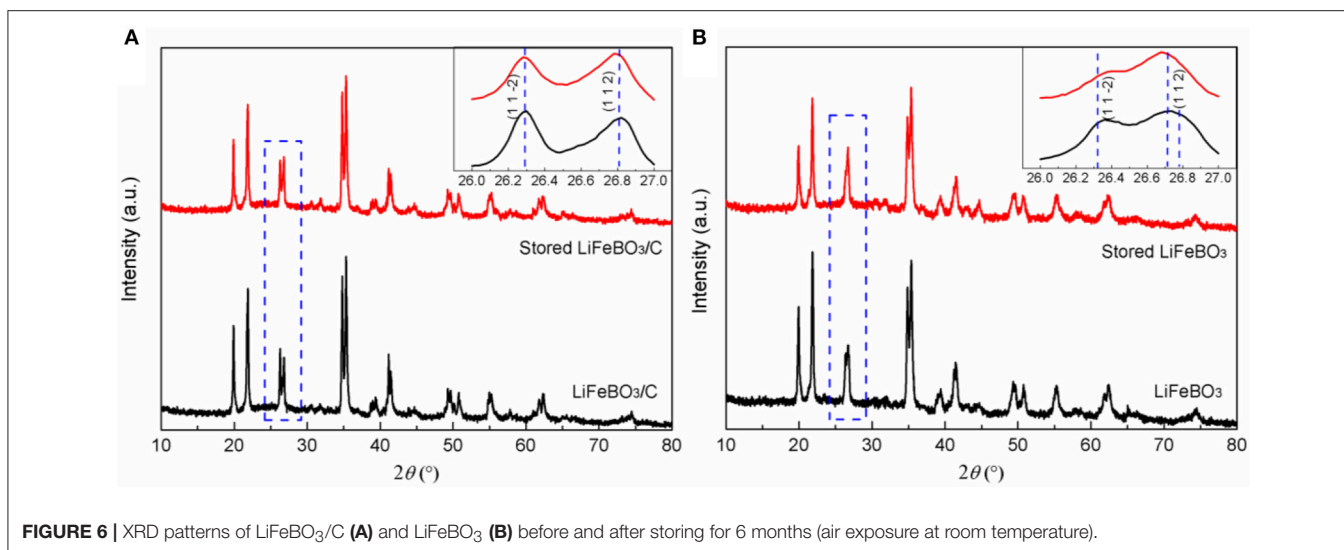


FIGURE 6 | XRD patterns of LiFeBO₃/C (A) and LiFeBO₃ (B) before and after storing for 6 months (air exposure at room temperature).

Figure 5A shows the cyclic voltammetry (CV) of the as-prepared LiFeBO₃/C and LiFeBO₃ samples. The oxidation/reduction peaks located at $\sim 2.95/2.35$ V correspond to the phase transition between LiFeBO₃ and FeBO₃. It is clearly observed that LiFeBO₃/C sample shows sharper peaks and larger areas than LiFeBO₃, implying the synthesized LiFeBO₃/C has a better reversibility. In addition, a couple of oxidation/reduction peaks are located at $\sim 2.09/1.85$ V, and these patterns can be ascribed to the degradation of LiFeBO₃ (Afyon et al., 2014).

In order to analyze the conductivity of the as-prepared LiFeBO₃/C and LiFeBO₃ samples, the EIS tests (**Figure 5B**) are measured in our study. Then the EIS data is fitted with Z-view software using an equivalent circuit, and the related parameters are listed in **Table 2**. R_s , Z_w , and R_{ct} in the equivalent circuit (insert **Figure 5B**) represent the resistance of the electrolyte, Warburg impedance and charge transfer resistance, respectively. The R_{ct} of LiFeBO₃/C (238.6 Ω) is lower than that of LiFeBO₃ (354.1 Ω), implying the charge transfer speed during the charge and discharge processes of electrode is significantly improved. The exchange current density (j_0) of synthesized LiFeBO₃/C and LiFeBO₃ is calculated by the following equation, respectively.

$$j_0 = \frac{RT}{nFR_{ct}}$$

Where T and n refer to the temperature and the electrons number, respectively. The exchange current density (j_0) of LiFeBO₃/C (10.78×10^{-4} mA cm⁻²) is higher than that of LiFeBO₃ (7.26×10^{-5} mA cm⁻²), which indicates that LiFeBO₃/C has a better electrode reaction reversibility than LiFeBO₃.

To evaluate the storage stability, LiFeBO₃/C and LiFeBO₃ samples were stored in air exposure for 6 months. XRD patterns of the LiFeBO₃/C and LiFeBO₃ samples before and after storage

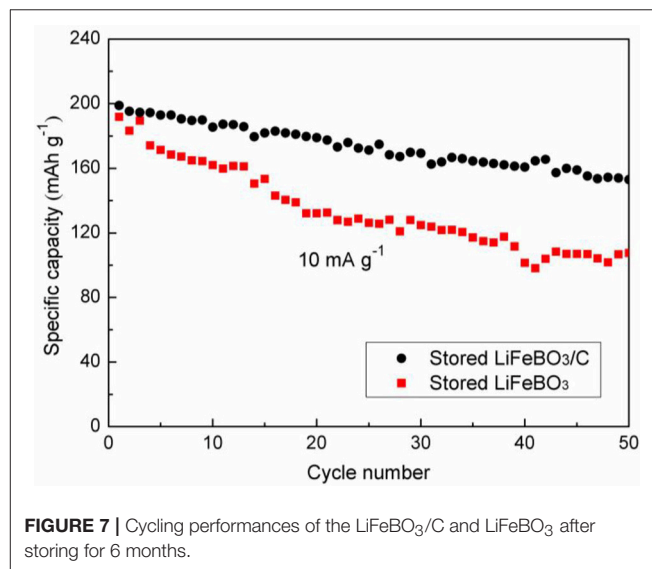


FIGURE 7 | Cycling performances of the LiFeBO₃/C and LiFeBO₃ after storing for 6 months.

are shown in **Figure 6**. Gratifyingly, the stored LiFeBO₃/C sample also remains its original crystal structure, verifying high storage stability of LiFeBO₃/C, as shown in **Figure 6A**. However, the XRD pattern of LiFeBO₃ changed after storing 6 months. As can be seen from **Figure 6B**, the intensity of (1 1 2) peak tends to increase while the intensity of (1 1 2) peak tends to decrease, and the two peaks prone to overlap each other. This phenomenon can be attributed to phase changing of LiFeBO₃ from monoclinic to orthorhombic structure with air corrosion (Bo et al., 2012; Chen et al., 2015).

After 6 months of storage, the cycling performances of LiFeBO₃/C and LiFeBO₃ samples are investigated, and the results are shown in **Figure 7**. The capacity of the stored LiFeBO₃/C is as high as 198.9 mAh g⁻¹ and there is 76.9% capacity retention after 50 cycles. However, the

stored LiFeBO₃ delivers a capacity of 191.7 mAh g⁻¹ and only 56.1% capacity retention after 50 cycles. Obviously, the stored LiFeBO₃/C shows higher stability and cycling performance than the stored LiFeBO₃. In summary, carbon coating and structural modification improve the conductivity of LiFeBO₃, shorten the Li⁺ diffusion/conduction path and protect LiFeBO₃ from moisture corrosion, thus leading to good electrochemical performance.

CONCLUSIONS

LiFeBO₃/C hollow sphere is successfully synthesized by a facile spray-drying method. Primary LiFeBO₃@C particles are connected by carbon layers and formed LiFeBO₃/C hollow spheres with improved electrical conductivity. Meanwhile, the hollow porous structure boosts the Li⁺ diffusion and the carbon layers of LiFeBO₃@C particles protect LiFeBO₃ from moisture corrosion. Therefore, the synthesized LiFeBO₃/C sample shows good electrochemical performances and improved storage performance. This work is conducive to obtaining promising and high-performance cathode materials for LIBs.

REFERENCES

- Afyon, S., Kundu, D., Krumeich, F., and Nesper, R. (2013). Nano-LiMnBO₃, a high-capacity cathode material for Li-ion batteries. *J. Power Sources* 224, 145–151. doi: 10.1016/j.jpowsour.2012.09.099
- Afyon, S., Mensing, C., Krumeich, F., and Nesper, R. (2014). The electrochemical activity for nano-LiCoBO₃ as a cathode material for Li-ion batteries. *Solid State Ionics* 256, 103–108. doi: 10.1016/j.ssi.2014.01.010
- Aravindan, V., and Umadevi, M. (2012). Synthesis and characterization of novel LiFeBO₃/C cathodes for lithium batteries. *Ionics* 18, 27–30. doi: 10.1007/s11581-011-0594-7
- Bo, S. H., Wang, F., Janssen, Y., Zeng, D. L., Nam, K. W., Xu, W. Q., et al. (2012). Degradation and (de)lithiation processes in the high capacity battery material LiFeBO₃. *J. Mater. Chem.* 22, 8799–8809. doi: 10.1039/c2jm16436a
- Chen, Z. X., Cao, L. F., Chen, L., Zhou, H. H., Zheng, C. M., Xie, K., et al. (2015). Mesoporous LiFeBO₃/C hollow spheres for improved stability lithium ion battery cathodes. *J. Power Sources* 298, 355–362. doi: 10.1016/j.jpowsour.2015.08.073
- Dong, Y. Z., Zhao, Y. M., Shi, Z. D., An, X. N., Fu, P., and Chen, L. (2008). The structure and electrochemical performance of LiFeBO₃ as a novel Li-battery cathode material. *Electrochim. Acta.* 53, 2339–2345. doi: 10.1016/j.electacta.2007.09.050
- Gu, X. F., Ting, M., and Zhi, S. (2017). Sol-gel synthesis of nanostructure LiFeBO₃/C lithium-ion cathode materials with high storage capacity. *J. Sol-Gel. Sci. Techn.* 81, 362–366. doi: 10.1007/s10971-016-4264-0
- Kalantarian, M. M., Asgari, S., and Mustarelli, P. (2013). A theoretical approach to evaluate the rate capability of Li-ion battery cathode materials. *J. Mater. Chem.* A 2, 107–115. doi: 10.1039/C3TA13387G
- Le Roux, B., Bourbon, C., Lebedev, O. I., Colin, J. F., and Pralong, V. (2015). Synthesis and characterization of the LiMnBO₃-LiCoBO₃ solid solution and its use as a lithium-ion cathode material. *Inorg. Chem.* 54, 5273–5279. doi: 10.1021/acs.inorgchem.5b00260
- Li, S. L., Xu, L. Q., Li, G. D., Wang, M., and Zhai, Y. J. (2013). *In-situ* controllable synthesis and performance investigation of carbon-coated monoclinic and hexagonal LiMnBO₃ composites as cathode materials in lithium-ion batteries. *J. Power Sources* 236, 54–60. doi: 10.1016/j.jpowsour.2013.02.027
- Li, Z., Wang, Y., Hu, Q., Yang, Y., Wu, Z., and Ban, C. (2015). Improved electrochemical performance of carbon-coated LiFeBO₃ nanoparticles

DATA AVAILABILITY

The raw data supporting the conclusions of this manuscript will be made available by the authors, without undue reservation, to any qualified researcher.

AUTHOR CONTRIBUTIONS

YS, ST, and WC did the main experiment and write the manuscript. LW and BW envolved the discussion of the experiment and revised the manuscript. HL and WL assisted the material synthesis. LW and SZ made the research plan. SZ and LW also provided the financial support.

FUNDING

This study was supported by the National Natural Science Foundation of China (51574168, 51574170, and 51774207), Guangxi Key Laboratory of Electrochemical and Magnetochemical Functional Materials (EMFM20182202), and Major Projects for Science & Technology Development of Guangxi Province, China (AA16380043).

- for lithium-ion batteries. *J. Nanosci. Nanotechnol.* 15, 7186–7190. doi: 10.1166/jnn.2015.10555
- Lin, Z. P., Zhao, Y. J., and Zhao, Y. M. (2012). First-principles study of the structural, magnetic, and electronic properties of LiMBO₃ (M=Mn, Fe, Co). *Phys. Lett. A* 376, 179–184. doi: 10.1016/j.physleta.2011.08.018
- Liu, Y., Xu, X., Wang, M., Lu, T., Sun, Z., and Pan, L. (2015). Nitrogen-doped carbon nanorods with excellent capacitive deionization ability. *J. Mater. Chem. A* 3, 17304–17311. doi: 10.1039/C5TA03663A
- Loftager, S., Garciaalstra, J. M., and Vegge, T. (2017). A density functional theory study of the carbon-coating effects on lithium iron borate battery electrodes. *Phys. Chem. Chem. Phys.* 19, 2087–2094. doi: 10.1039/C6CP06312H
- Lutterotti, L. (2011). *Maud version 2.91*. Avliable online at: <https://www.softpedia.com/get/Science-CAD/Maud.shtml> (accessed March, 2019)
- Ma, T., Muslim, A., and Su, Z. (2015). Microwave synthesis and electrochemical properties of lithium manganese borate as cathode for lithium ion batteries. *J. Power Sources* 282, 95–99. doi: 10.1016/j.jpowsour.2015.02.013
- Michalski, P. P., Pietrzak, T. K., Nowinski, J. L., Wasiucionek, M., and Garbarczyk, J. E. (2017). Novel nanocrystalline mixed conductors based on LiFeBO₃ glass. *Solid State Ionics* 302, 40–44. doi: 10.1016/j.ssi.2016.12.002
- Moskon, J., Pivko, M., Jerman, I., Tchernychova, E., Zabukovec Logar, N., Selih, V. S., et al. (2016). Cycling stability and degradation mechanism of LiMnPO₄ based electrodes. *J. Power Sources* 303, 97–108. doi: 10.1016/j.jpowsour.2015.10.094
- Nayak, P. K., Yang, L., Brehm, W., and Adelhelm, P. (2018). From Lithium-ion to sodium-ion batteries: advantages, challenges, and surprises. *Angew. Chem. Int. Edit.* 57, 102–120. doi: 10.1002/anie.201703772
- Rietveld, H. M. (1967). Line profiles of neutron powder-diffraction peaks for structure refinement. *Acta Cryst.* 22, 151–152. doi: 10.1107/S0365110X67000234
- Sin, B. C., Singh, L., Lee, K. E., Kim, M., Cho, M., Yarger, J. L., et al. (2015). Enhanced electrochemical performance of LiFe_{0.4}Mn_{0.6}(PO₄)_{1-x}(BO₃)_x as cathode material for lithium ion batteries. *J. Electroanal. Chem.* 756, 56–60. doi: 10.1016/j.jelechem.2015.08.012
- Tang, A. P., He, D. H., He, Z. Q., Xu, G. R., Song, H. S., and Peng, R. H. (2015). Electrochemical performance of LiMnBO₃/C composite synthesized by a combination of impregnation and precipitation followed by annealing. *J. Power Sources* 275, 888–892. doi: 10.1016/j.jpowsour.2014.11.087

- Tao, L., Neilson, J. R., Melot, B. C., Mcqueen, T. M., Masquelier, C., and Rouse, G. (2013). Magnetic structures of LiMBO₃ (M = Mn, Fe, Co) lithiated transition metal borates. *Inorg. Chem.* 52, 11966–11974. doi: 10.1021/ic401671m
- Wu, L., Zheng, J., Wang, L., Xiong, X., Shao, Y., Wang, G., et al. (2019). PPy-encapsulated SnS₂ nanosheets stabilized by defects on a TiO₂ support as a durable anode material for lithium-ion batteries. *Angew. Chem. Int. Edit.* 58, 811–815. doi: 10.1002/anie.201811784
- Yang, H., Wu, H. H., Ge, M., Li, L., Yuan, Y., Yao, Y., et al. (2019). Simultaneously dual modification of Ni-rich layered oxide cathode for high-energy lithium-ion batteries. *Adv. Funct. Mater.* 29:1808825. doi: 10.1002/adfm.201808825
- Zhang, B., Ming, L., Zheng, J. C., Zhang, J. F., Shen, C., Han, Y. D., et al. (2014). Synthesis and characterization of multi-layer core-shell structural LiFeBO₃/C as a novel Li-battery cathode material. *J. Power Sources* 261, 249–254. doi: 10.1016/j.jpowsour.2014.03.082
- Zhang, B., Zhu, Y. S., Yu, W. J., Zhang, J. F., and An, C. S. (2017). Facile synthesis of carbon-encapsulated LiMnBO₃ composite by the sol-gel method as a lithium-ion battery cathode material. *J. Alloys. Compd.* 704, 343–347. doi: 10.1016/j.jallcom.2017.02.058
- Zheng, J. C., Yang, Z., He, Z. J., Tong, H., Yu, W. J., and Zhang, J. F. (2018a). In situ formed LiNi_{0.8}Co_{0.15}Al_{0.05}O₂@Li₄SiO₄ composite cathode material with high rate capability and long cycling stability for lithium-ion batteries. *Nano Energy* 53, 613–621. doi: 10.1016/j.nanoen.2018.09.014
- Zheng, J. C., Yang, Z., Wang, P. B., Tang, L. B., An, C. S., and He, Z. J. (2018b). Multiple linkage modification of lithium-rich layered oxide Li_{1.2}Mn_{0.54}Ni_{0.13}Co_{0.13}O₂ for lithium ion battery. *ACS Appl. Mater. Inter.* 10, 31324–31329. doi: 10.1021/acsami.8b09256
- Zhu, Y. E., Yang, L. P., Sheng, J., Chen, Y. N., Gu, H. C., Wei, J. P., et al. (2017). Fast sodium storage in TiO₂@CNT@C nanorods for high-performance Na-ion capacitors. *Adv. Energy Mater.* 7:1701222. doi: 10.1002/aenm.201701222

Conflict of Interest Statement: The authors declare that the research was conducted in the absence of any commercial or financial relationships that could be construed as a potential conflict of interest.

Copyright © 2019 Sui, Chen, Tang, Wu, Wang, Li, Li and Zhong. This is an open-access article distributed under the terms of the Creative Commons Attribution License (CC BY). The use, distribution or reproduction in other forums is permitted, provided the original author(s) and the copyright owner(s) are credited and that the original publication in this journal is cited, in accordance with accepted academic practice. No use, distribution or reproduction is permitted which does not comply with these terms.